DOI: 10.1557/adv.2019.16

Transport and Electromechanical Properties of $Ca_3TaGa_3Si_2O_{14}$ Piezoelectric Crystals at Extreme Temperatures

Yuriy Suhak[1], Ward L. Johnson[2], Andrei Sotnikov[3], Hagen Schmidt[3], Holger Fritze[1]

[1]*Clausthal University of Technology, Am Stollen 19B, Goslar, 38640, Germany.*

[2]*National Institute of Standards and Technology, 325 Broadway St., Boulder, CO 80305, U.S.A.*

[3]*Leibniz Institute for Solid State and Materials Research Dresden, Helmholtzstr. 20, Dresden, 01069, Germany.*

ABSTRACT

Transport mechanisms in structurally ordered piezoelectric $Ca_3TaGa_3Si_2O_{14}$ (CTGS) single crystals are studied in the temperature range of 1000-1300 °C by application of the isotope ^{18}O as a tracer and subsequent analysis of diffusion profiles of this isotope using secondary ion mass spectrometry (SIMS). Determined oxygen self-diffusion coefficients enable calculation of oxygen ion contribution to the total conductivity, which is shown to be small. Since very low contributions of the cations have to be expected, the total conductivity must be dominated by electron transport. Ion and electron conductivities are governed by different mechanisms with activation energies (1.9±0.1) eV and (1.2±0.07) eV, respectively. Further, the electromechanical losses are studied as a function of temperature by means of impedance spectroscopy on samples with electrodes and a contactless tone-burst excitation technique. At temperatures above 650 °C the conductivity-related losses are dominant. Finally, the operation of CTGS resonators is demonstrated at cryogenic temperatures and materials piezoelectric strain constants are determined from 4.2 K to room temperature.

INTRODUCTION

Piezoelectric components have broad potential for applications at extreme temperatures. For example, the mass sensitivity of resonant sensors at high temperatures

offers advantages for sensing gases or soot particles and thus supports the increase in efficiency and environmental compatibility of energy conversion processes [1]. However, application of piezoelectric materials at elevated temperatures faces many challenges, including thermal instability of the dielectric, piezoelectric and electromechanical properties, increased damping, and chemical instability (decomposition, oxidation). Additionally, the applicability of these materials for low temperature operation properties is of particular importance.

Piezoelectric crystals of the langasite (LGS, $La_3Ga_5SiO_{14}$) family are recognized as excellent candidates for low and high temperature applications as these crystals can be piezoelectrically excited from cryogenic temperatures to 1300 °C or more. They have been shown to have a high degree of thermal stability [2,3], which enables their application as gravimetric sensors [4-6]. CTGS ($Ca_3TaGa_3Si_2O_{14}$) is a relatively new compound of the langasite family, which has a fully ordered structure with lower conductivity and damping than LGS [7-9].

This work focuses on characteristics of CTGS as a function of temperature. In particular, investigations of atomic transport mechanisms in CTGS are carried out at temperatures up to 1300 °C and correlated with electrical properties. Further, electromechanical losses are analyzed as a function of temperature from ambient room temperature (RT) up to 900 °C. Finally, the piezoelectric strain constants of CTGS are determined in the temperature range from 4.2 K to RT.

EXPERIMENTAL METHODS

CTGS crystals used in this study were grown by the Czochralski technique. Transport mechanisms and electrical properties were investigated on crystals provided by the Institute for Crystal Growth (IKZ), Berlin, Germany. Ultrasonic pulse-echo experiments were performed on crystals grown by Fomos-Materials, Moscow, Russia [10]. Electromechanical losses were studied with acoustic resonance techniques on both Fomos and IKZ crystals.

In order to investigate atomic transport mechanisms in CTGS, oxygen self-diffusion is studied, because O is expected to be the most mobile atomic species in the crystal lattice [11]. These experiments were performed using the stable tracer isotope ^{18}O by annealing the samples in an $^{18}O_2$ enriched atmosphere (90 % $^{18}O_2$, 200 mbar). Subsequently the ^{18}O depth profiles were analysed by secondary ion mass spectrometry (SIMS) (Hiden Analytical). Prior to each diffusion run, each sample was pre-annealed in air to equilibrate it. Table 1 summarizes pre-annealing and $^{18}O_2$-annealing temperatures and times for different CTGS samples. The diffusion runs were performed twice at some temperatures to validate the results. The methods of the diffusion experiments are described in more detail in [9].

Table 1. Annealing temperatures and times for CTGS samples

Annealing Temperature	Pre-Annealing Time	$^{18}O_2$-Annealing Time
1000 °C	192 h	48 h
1100 °C	96 h	24 h
1150 °C	72 h	18 h
1200 °C	48 h	12 h
1250 °C	32 h	8 h
1300 °C	16 h	4 h

Measurements of the electrical conductivity as a function of temperature were performed on Y-cut CTGS plates (10 mm×10 mm×0.5 mm) using an impedance analyser (Solartron 1260). The samples were coated with platinum electrodes that were deposited

by a screen-printing technique. From the impedance plots the bulk resistance was extracted by fitting the spectra to an electrical-circuit model consisting of a constant phase element connected in parallel with a bulk resistance.

Electromechanical losses were studied by two independent methods, impedance spectroscopy and contactless tone-burst excitation, on Y-cut disc resonators with diameters 14 mm and fundamental frequencies of approximately 5.8 MHz (Fomos) and 4.5 MHz (IKZ). The crystal holder, electrodes, data acquisition and analysis, electronic system and methods employed in these measurements are described elsewhere [12, 13].

Ultrasonic experiments were performed on X-, Y-, Z- and rotated by ±45° around X bars (7 mm × 7 mm × 7 mm) and plates (10 mm × 10 mm × 0.5 mm) with a RITEC RAM-5000 and UTEX UT340 measurement systems. Bulk acoustic waves (BAWs) were excited and received using Y+36°- and X-cut $LiNbO_3$ transducers for longitudinal and shear modes, respectively, by applying short driving voltage bursts (RAM-5000) or spike-shaped pulses (UT340). For piezoelectrically active cuts (X-, Y- and ±45°), sound excitation and receiving were done through the intrinsic piezoelectric effect of the crystal. BAW velocities were determined from the time delay between consistent echo-signals. Piezoelectric stress constants e_{11} and e_{14} were derived using a set of relations between velocities of different BAW modes and the material constants of the crystal [14].

RESULTS AND DISCUSSION

Atomic transport

To analyse oxygen self-diffusion, the secondary ion intensities I of ^{16}O and ^{18}O were recorded by SIMS as a function of sputtering time. Since these O isotopes are chemically identical, the intensity of the signal was converted to the ^{18}O atomic fraction c according to $c = [I(^{18}O)]/[I(^{16}O)+I(^{18}O)]$. Subsequently, the crater depth was determined by the profilometry, enabling presentation of ^{18}O atomic fraction as a function of diffusion depth d if a constant sputter rate is assumed. Figure 1 shows example of results for the normalized oxygen concentration as a function of d for a CTGS sample annealed in ^{18}O at 1000 °C for 48 hours. Fitting an analytical solution of Fick's second law to the concentration depth profiles allows extraction of the oxygen diffusion coefficients D in CTGS, which are shown in Figure 2. The fitting procedure is described in detail in [11].

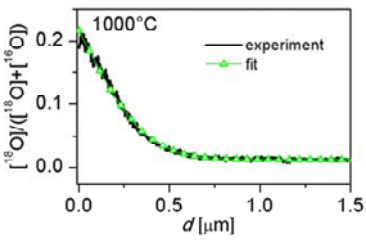

Fig. 1: ^{18}O diffusion profile in CTGS annealed in an $^{18}O_2$-atmosphere for 48 hours at 1000 °C and corresponding fit (see text for details).

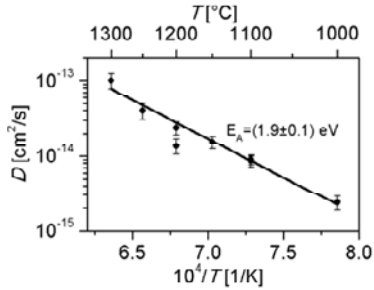

Fig. 2: Oxygen diffusion coefficients obtained for CTGS as a function of reciprocal temperature.

The data in Figure 2 are generally consistent with a constant slope of log(D) vs $1/T$, indicating that oxygen diffusion is controlled by a single thermally activated mechanism over the entire measured temperature range. However, some differences in measured D and the fit line are observed at 1200 °C. These differences could possibly be caused by spatial variations in properties within a crystal boule. Consequently, additional measurements are required to reliably determine the diffusion coefficients at this temperature. From the fit in Figure 2, the Arrhenius equation $D(T) = D_0 \exp(-E_A/kT)$ yields an activation energy E_A of (1.9 ± 0.1) eV. Note, that a smaller value for E_A was reported in a preliminary study [9]. In that study, the maximum temperature of the measurements was 1200 °C and only three data points were available, which limited the accuracy of the value obtained for E_A. Consequently, the difference is attributed solely to the measurement error of the previous measurements.

The contribution σ_0 of oxygen transport to the total electrical conductivity is calculated from the following expression [15,16]:

$$\sigma_O = \frac{(2q)^2}{kT}[O_O]D \,, \qquad (1)$$

where $2q$ and $[O_O]$ are the charge of the mobile species and the oxygen concentration, respectively. This contribution is compared in Figure 3 to the bulk electrical conductivity σ_B of CTGS, as determined by impedance spectroscopy. As shown in this figure, the oxygen ion contribution is a small part of the conductivity over the entire measured temperature range. At 1000 °C, it is only about 80 ppm of the total conductivity and, at the highest measured temperature, it reaches 200 ppm. The many data points for σ_B in Figure 3 provide compelling evidence for one thermally activated process with an activation energy of (1.2 ± 0.07) eV being dominant over the entire measured temperature range. Different activation energies for bulk and ionic conductivities indicate that those processes are governed by different mechanisms. Considering that contributions of other cations to the total conductivity are expected to be even smaller than that determined here for O [11], one can conclude that electronic conduction mechanism is the dominant contribution to σ_B in the whole measured temperature range.

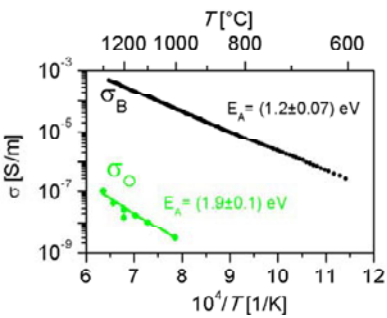

Fig. 3: Total bulk and oxygen ion conductivities in CTGS as a function of reciprocal temperature.

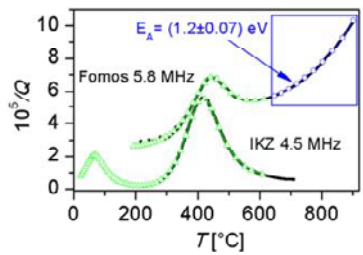

Fig. 4: Measured $Q^{-1}(T)$ values and corresponding fits for IKZ and Fomos sample. (See text for details)

Electromechanical losses

Figure 4 presents the inverse quality factor Q^{-1} (acoustic loss) as a function of temperature for the 5.8 MHz (Fomos) and 4.5 MHz (IKZ) CTGS resonators determined,

respectively, from impedance spectroscopy and time-domain measurements of exponential decay following tone-burst excitation. The overall higher level of Q^{-1} of the Fomos resonator is attributed to greater contributions to the loss from contact excitation than from contactless excitation (IKZ). The loss peaks in the IKZ resonator near 80 °C and 420 °C, as well as the peak in the Fomos resonator near 450 °C, are attributed to anelastic relaxation of point defects. The anelastic relaxations are dependent on the measurement temperature and frequency [17, 9], and the higher temperature of the peak maximum in the Fomos specimen is understood to arise from the resonant frequency for these measurements being higher (5.8 MHz) than that for the IKZ specimen (4.5 MHz). Fits of $Q^{-1}(T)$ to a model function up to 600 °C were performed in our previous report [9] and are also shown in Figure 4 (triangles).

At sufficiently elevated temperatures (i.e., above 650 °C) the losses are dominated by piezoelectric/conductivity relaxation. This contribution is dependent on frequency and temperature and can be approximated by [18, 19]

$$Q_c^{-1}(\omega,T) \approx K^2 \frac{\omega\tau_c}{1+\omega^2\tau_c^2}, \qquad (2)$$

where, K^2 and τ_c are the electromechanical coupling coefficient and the dielectric relaxation time, respectively, with $\tau_c = \varepsilon / \sigma$. Here, σ is the electrical conductivity and ε is the dielectric constant. The measured Q^{-1} data for the Fomos resonator were fitted to Eq. 2 and the results of this fit are shown in Figure 4 (blue circles). The activation energy for piezoelectric/conductivity relaxation mechanism is found to be (1.2 ± 0.07) eV, which matches the activation energy determined from the bulk conductivity (Figure 3). Therefore, these results provide compelling evidence that the measured acoustic loss above 650 °C in this specimen is dominated by piezoelectric/conductivity relaxation.

Piezoelectric constants

As described in Experimental Methods, BAW velocities for several crystal orientations were measured with burst and spike-shaped pulsed excitation followed by time-domain signal analysis. Typical signals for a Y-cut crystal at room temperature and 4.2 K are shown in Figure 5. As illustrated in this figure, the acoustic attenuation was found to be lower at 4.2 K than at room temperature.

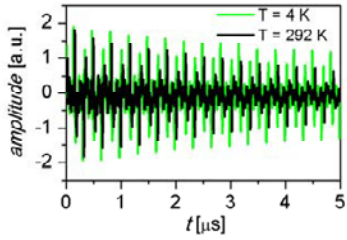

Fig. 5: Ultrasonic pulse-echo pattern for the Y-cut CTGS single crystal at 292 K and 4.2 K.

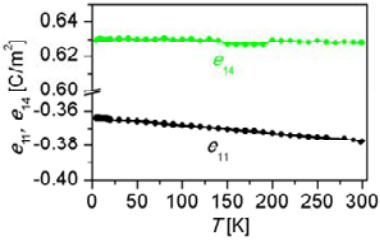

Fig. 6: Piezoelectric constants e_{11} and e_{14} as a function of temperature.

Piezoelectric constants e_{11} and e_{14} as a function of temperature in the range of 4.2-292 K are plotted in Figure 6. In comparison, reported values for quartz at RT are (0.15 – 0.17) C/m^2 for e_{11} and -(0.06 – 0.04) C/m^2 for e_{14} [20]. For LGS, e_{11} is reported to be -0.41 C/m^2 at 4.2 K and -0.43 C/m^2 at RT, and e_{14} is reported to be 0.091 C/m^2 at

4.2 K and 0.089 C/m^2 at RT [21]. The RT value of e_{11} for CTGS (the constant that determines the coupling strength for Y-cut resonators) is, therefore, more than two times that of quartz and approximately 8 % less than that of LGS.

CONCLUSIONS

In summary, the properties of CTGS have been investigated in a broad temperature range from cryogenic temperatures to about 1300 °C. In particular, the transport mechanisms in CTGS single crystals in the range of 1000-1300 °C are found to be correlated with electrical and electromechanical properties. Even at the highest temperatures, the electronic contribution to the conductivity is found to be dominant in CTGS, while the contribution of conductivity from oxygen transport is only about 200 ppm of the overall conductivity. Further, analysis of high-temperature electromechanical losses in CTGS reveals that, at temperatures above 650 °C, the losses are dominated by piezoelectric/conductivity relaxation, since the activation energies obtained for the conductivity and loss are the same. It was shown that the CTGS resonators can be operated at cryogenic temperatures. The piezoelectric strain constants were determined as a function of temperature from 4.2 K to 293 K. The constant e_{11}, which determines the coupling strength of Y-cut resonators, is found to be slightly less than that of LGS over the measured temperature range and more than a factor of two greater than that of quartz at ambient temperatures.

ACKNOWLEDGEMENTS

A research grant from the German Research Foundation (DFG: FR 1301/21-1 and SO 1085/2-1) supported this work. Further, the authors from Clausthal University of Technology acknowledge the support of the Energie-Forschungszentrum Niedersachsen, Goslar, Germany. This manuscript is a contribution of the National Institute of Standards and Technology and is not subject to copyright in the United States.

References:

[1] X. Jiang, K. Kim, S. Zhang, J. Johnson, G. Salazar, Sensors **14**, 144 (2014).
[2] H. Fritze, M. Schulz, H. Seh, H. L. Tuller, Mater. Res. Soc. Symp. Proc. **835**, A3.9.1 (2005).
[3] H. Fritze, M. Schulz, H. Seh, H. L. Tuller, Solid State Ionics **177**, 2313 (2006).
[4] H. Fritze, H. L. Tuller, U.S. Patent No. 6.370.955 (2002).
[5] H. Seh, H. L. Tuller, H. Fritze, J. Eur. Ceram. Soc. **24**, 1425 (2004).
[6] S. Schröder, H. Fritze, S. Bishop, D. Chen, H.L. Tuller, Appl. Phys. Lett. **112**, 213502 (2018).
[7] H. Ohsato, T. Iwataki, H. Morikoshi, Trans. Electr. Electron. Mater. **13**, 171 (2012).
[8] S. Zhang, Y. Zheng, H. Kong, J. Xin, E. Frantz, T.R. Shrout, J. Appl. Phys. **105**, 114107 (2009).
[9] Yu. Suhak, M. Schulz, W. L. Johnson, A. Sotnikov, H. Schmidt, H. Fritze, Solid State Ionics **317**, 221 (2018).
[10] Certain trade names and company products are identified in this paper to adequately describe experimental methods. Such identification does not imply recommendation or endorsement by the National Institute of Standards and Technology, nor does it imply that the products are necessarily the best for the purpose.
[11] M. Schulz, H. Fritze, H. L. Tuller, H. Seh, IEEE Trans. Ultrason., Ferroelect., Freq. Control., **51**, 1381 (2004).
[12] W. L. Johnson, M. Schulz, H. Fritze, IEEE Trans. Ultrason., Ferroelect., Freq. Control. **61**, 1433 (2014).
[13] H. Fritze, Meas. Sci. Technol. **22**, 12002 (2011).
[14] A. Sotnikov, H. Schmidt, M. Weihnacht, O. Busanov, S. Sakharov, Proc. IEEE Int. Ultrason. Symp., pp. 1688-1691 (2013).
[15] H. Fritze, J. Electroceram., **26**, 122 (2011).

[16] P.G. Shewmon, *Diffusion in Solids* (McGraw-Hill, New York, 1963).
[17] A.S. Nowick, B.S. Berry, *Anelastic relaxation in crystalline solids* (Academic Press, New York, 1972).
[18] W.L. Johnson, S.A. Kim, S. Uda, C.F. Rivenbark, J. Appl. Phys, **110**, 123528 (2011).
[19] A. R. Hutson, D. L. White, J. Appl. Phys., **33**, 40 (1962).
[20] H. Ogi, T. Ohmori, N. Nakamura, and M. Hirao, J. Appl. Phys. **100**, 053511 (2006).
[21] M.Weihnacht, A. Sotnikov, H. Schmidt, B. Wall, R. Grünwald, Proc. IEEE Ultrason. Symp., pp. 1549-1552 (2012).